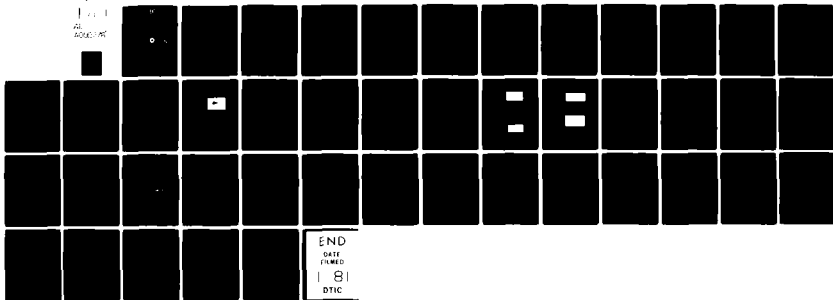


AD-A092 276

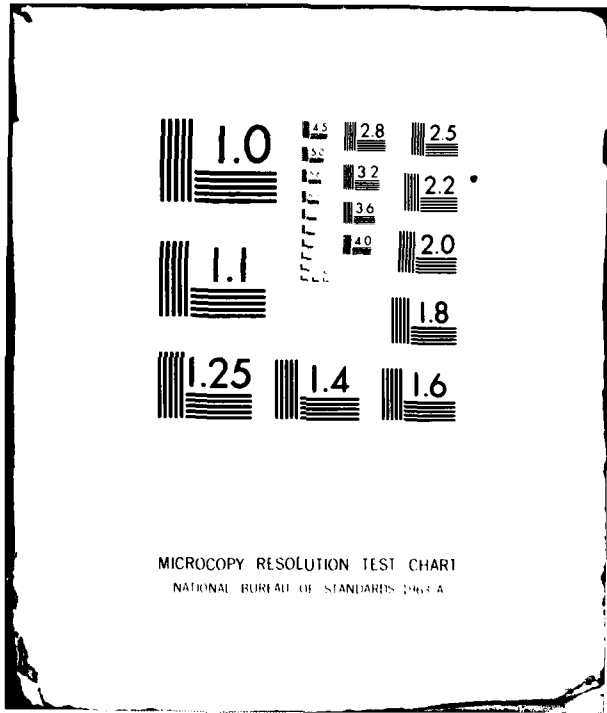
NATIONAL OCEANIC AND ATMOSPHERIC ADMINISTRATION BOUL--ETC F/8 17/9
EVALUATION OF A METEOROLOGICAL AIRBORNE PULSE DOPPLER RADAR.(U)
JUL 80 B L TROTTER, R G STRAUCH, C L FRUSH DOT-FA78WAI-877
FAA-RD-80-98 NL

UNCLASSIFIED

ALL INFORMATION CONTAINED
HEREIN IS UNCLASSIFIED



END
DATE
FILMED
1 81
DTIC



MICROCOPY RESOLUTION TEST CHART
NATIONAL BUREAU OF STANDARDS 1963-A

Report No. FAA-RD-80-98

LEVEL *III*

12

**EVALUATION OF A METEOROLOGICAL
AIRBORNE PULSE DOPPLER RADAR**

AD A092276

**B.L. Trotter
NOAA/ERL/Weather Modification Program Office
Boulder, Colorado 80303**

**R.G. Strauch
NOAA/ERL/Wave Propagation Laboratory
Boulder, Colorado 80303**

**C.L. Frush
National Center for Atmospheric Research
Boulder, Colorado 80303**



**DTIC
ELECTRA
DEC 1 1980**

**July 1980
Final Report**

Document is available to the U.S. public through
the National Technical Information Service,
Springfield, Virginia 22161.

DDC FILE COPY

**Prepared for
U.S. DEPARTMENT OF TRANSPORTATION
FEDERAL AVIATION ADMINISTRATION
Systems Research & Development Service
Washington, D.C. 20590**

80 11 28 015

NOTICE

This document is disseminated under the sponsorship of the Department of Transportation in the interest of information exchange. The United States Government assumes no liability for its contents or use thereof.

Technical Report Documentation Page

1. Report No. 18 FAA-RD-80-98	2. Government Accession No. AD-A092 276	3. Recipient's Catalog No.	
4. Title and Subtitle 6 EVALUATION OF A METEOROLOGICAL AIRBORNE PULSE DOPPLER RADAR.		5. Report Date 11 Jul 1980	6. Performing Organization Code RX9
7. Author(s) 10 B. L. Trotter R. G. Strauch C. L. Frush		8. Performing Organization Report No. 12 47	
9. Performing Organization Name and Address National Oceanic & Atmospheric Administration Environmental Research Laboratories Weather Modification Program Office--RX9 325 Broadway, Boulder, CO 80303		10. Work Unit No. (TRAIS)	11. Contract or Grant No. DOT-FA78WAI-877
12. Sponsoring Agency Name and Address U.S. Department of Transportation Federal Aviation Administration Systems Research & Development Service Washington, D.C. 20590		13. Type of Report and Period Covered Phase I Final report Oct 1977 to July 1980 14. Sponsoring Agency Code ARD-451	
15. Supplementary Notes			
16. Abstract An X-Band airborne radar has been modified to provide a Doppler radar capability. The Doppler radar has been tested to prove the system concept usable. Tests were conducted at Norman, Oklahoma, from May 30 to June 9 of 1978 and in Miami, Florida, on December 1 through December 5, 1979. Optimally the tests would have used meteorological targets for measurement of radial velocities, however, most tests had to be conducted with chaff and ground returns. The tests did show that the airborne Doppler radar will measure velocities that are comparable to those measured by a ground based Doppler radar and those that can be computed by a high accuracy inertial navigation system. The error in the measured radial velocities, when compared to other sensors, is much less than the estimated RMS error of 2 meters/second.			
17. Key Words Airborne Doppler Radar Radial Velocity Doppler Meteorological Doppler		18. Distribution Statement Document is available to the U.S. public through the National Technical Information Service, Springfield, Virginia 22161.	
19. Security Classif. (of this report) unclassified	20. Security Classif. (of this page) unclassified	21. No. of Pages 39	22. Price

406502

METRIC CONVERSION FACTORS

Symbol	When You Know	Multiply by	To Find	Symbol
LENGTH				
in	inches	2.5	centimeters	cm
ft	feet	30	centimeters	cm
yd	yards	0.9	meters	m
mi	miles	1.6	kilometers	km
AREA				
sq ft	square inches	6.5	square centimeters	cm ²
sq ft	square feet	0.09	square meters	m ²
sq yd	square yards	0.8	square meters	m ²
sq mi	square miles	2.6	square kilometers	km ²
	acres	0.4	hectares	ha
MASS (weight)				
oz	ounces	28	grams	g
lb	pounds	0.45	kilograms	kg
	short tons (2000 lb)	0.9	tonnes	t
VOLUME				
cup	cup	5	milliliters	ml
fl oz	fluid ounces	30	milliliters	ml
c	cup	0.24	liters	l
pt	pint	0.47	liters	l
qt	quart	0.95	liters	l
gal	gallon	3.8	liters	l
cu ft	cubic feet	0.03	cubic meters	m ³
cu yd	cubic yards	0.76	cubic meters	m ³
TEMPERATURE (exact)				
°F	Fahrenheit temperature	5/9 (after subtracting 32)	Celsius temperature	°C

*1 in = 2.54 exactly. For other exact conversions and more exact tables, see NBS Mon. Publ. 160, Units of Weights and Measures, Price \$2.25, SD Catalog No. 111-10, 296.

Symbol	When You Know	Multiply by	To Find	Symbol
LENGTH				
mm	millimeters	0.04	inches	in
cm	centimeters	0.4	inches	in
m	meters	3.3	feet	ft
mi	miles	1.1	yards	yd
km	kilometers	0.6	miles	mi
AREA				
cm ²	square centimeters	0.16	square inches	in ²
m ²	square meters	1.2	square yards	yd ²
km ²	square kilometers	0.4	square miles	mi ²
ha	hectares (10,000 m ²)	2.5	acres	ac
MASS (weight)				
g	grams	0.035	ounces	oz
kg	kilograms	2.2	pounds	lb
t	tonnes (1000 kg)	1.1	short tons	st
VOLUME				
ml	milliliters	0.03	fluid ounces	fl oz
l	liters	2.1	pints	pt
l	liters	1.06	quarts	qt
m ³	cubic meters	0.26	gallons	gal
m ³	cubic meters	35	cubic feet	ft ³
m ³	cubic meters	1.3	cubic yards	yd ³
TEMPERATURE (exact)				
°C	Celsius temperature	9/5 (then add 32)	Fahrenheit temperature	°F

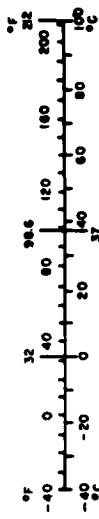


TABLE OF CONTENTS

	Page
1.0 Radar System Description	1
2.0 Airborne Doppler Error Sources	4
2.1 Transmitting and Receiving System Instabilities	4
2.2 Internal Stability Requirements	7
2.3 External Stability Requirements	9
3.0 Test Program	13
3.1 Test Description and Results	13
4.0 Conclusions	25
5.0 Recommendations	26

Acceptance For	
NTIS	<input checked="" type="checkbox"/>
ERIC	<input type="checkbox"/>
Unannounced	<input type="checkbox"/>
Justification	<input type="checkbox"/>
Distribution/	
Availability Codes	
Dist	Avail and/or Special
A	

LIST OF ILLUSTRATIONS

		Page
Figure 1	Block Diagram of Complete Radar System	2
Figure 2	Single Transmitted Pulse Mixed with Stable	10
Figure 3a, 3b	Bipolar Video of Grand Returns Repetitive Transmissions	15
Figure 4a	Noise Level With No RF Returns	16
Figure 4b	Doppler Spectrum of Snow Flakes with Increased Noise	16
Figure 5	Race Track Patterns	17
Figure 6	Doppler Data Fields (Airborne and Ground Radars)	21
Figure 7	Velocity Spectrum of Rain	22
Figure 8	Range Velocity Spectrum of Chaff and Cloud	23

LIST OF TABLES

Table 1	Radar Characteristics	3
---------	-----------------------	---

LIST OF GRAPHS

Graph 1	Percent Frequency Change in Transmitted Pulse vs. Time	28
Graph 2	Measured Vertical Velocities	29
Graph 2a	Ground Clutter Velocity vs. Antenna Position	30
Graph 3	Aircraft Track During Chaff Drop	31
Graph 4	Wind Speed Measured by Aircraft During Chaff Drop	32
Graph 5	Chaff Drop in Oklahoma	33
Graph 6	Wind Speed Data	34
Appendix I	Description of the National Center for Atmospheric Research Data System	35

1.0 Radar System Description

The airborne Doppler radar is a modified version of the X-band radar that is installed in the tail section of the WP3D aircraft. The characteristics of the basic radar are shown in Table 1. Reference to Figure 1 should be made for the following description. The transmitter power amplifier used in the radar is a magnetron. It was determined that the intra-pulse frequency stability of the magnetron was satisfactory for use in the configuration of this radar. The intra-pulse frequency change of the magnetron is small as compared to the inter-pulse frequency changes. A sample of the transmitted RF signal is attenuated through a RF coupler and sent to a mixer preamplifier. A second input to the mixer preamplifier is a signal from a stable oscillator. The frequency of the stable oscillator is selectable in order to maintain an approximate 30 MHz intermediate frequency (IF) signal from the mixer. The IF signal from the mixed preamplifier is applied to the coherent oscillator by way of an isolation amplifier. The coherent oscillator has as a second input a trigger signal that when applied to the magnetron produces the transmitted 0.5 microsecond burst of RF energy. The coherent oscillator circuit detects the first positive going transition of the magnetron output mixed to 30 MHz after the occurrence of the radar trigger. The detected signal causes the oscillator to produce an output that will be at a frequency of 30 MHz and starts at the same phase point of the input signal to the oscillator for each transmitted signal. The oscillator will continue to oscillate during the interpulse period until it is turned off. A signal internally generated in the oscillator circuit turns the oscillator off after all useful echos have been received. By

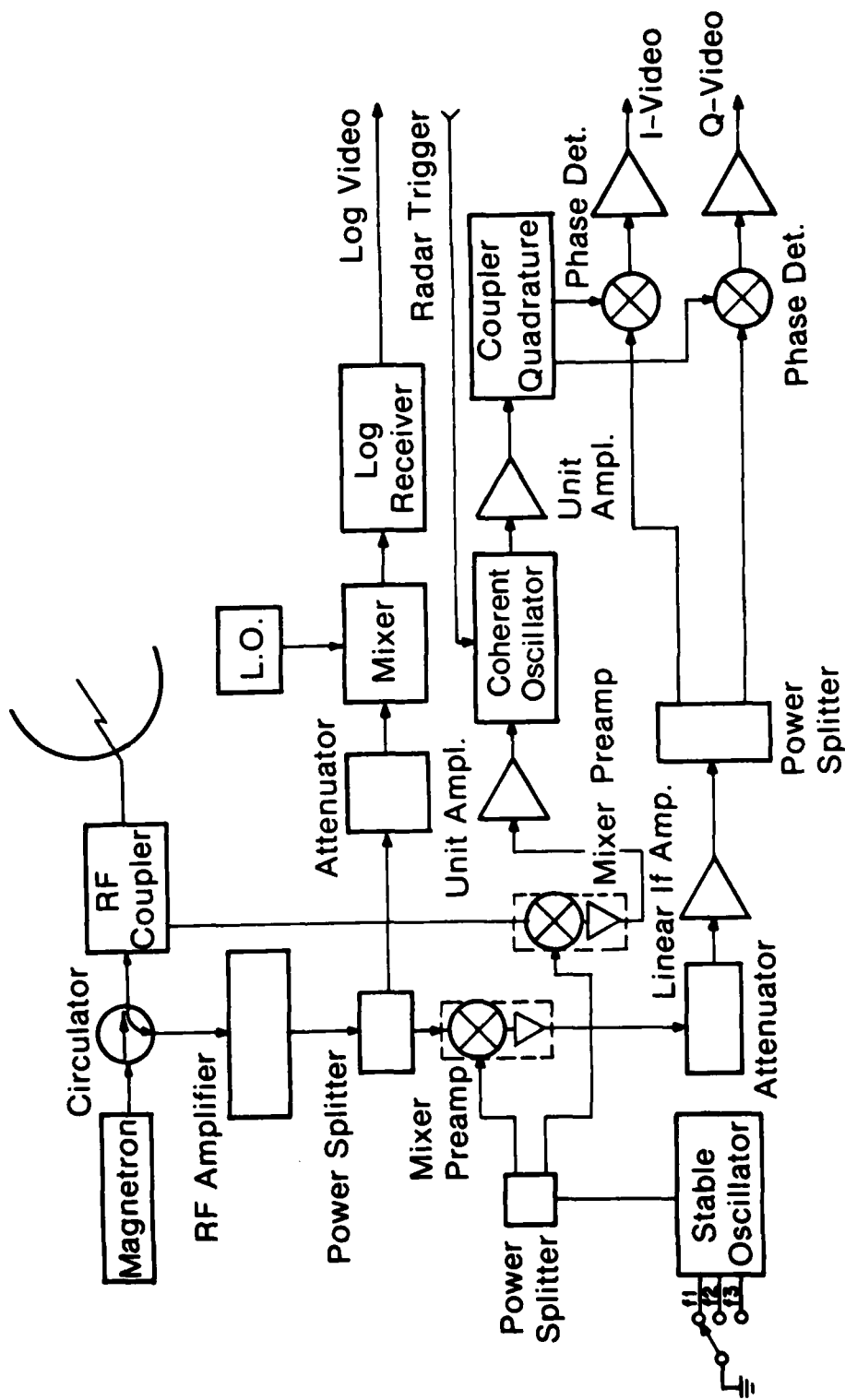


Figure 1. Block Diagram of Radar System

Transmitter Frequency	9315 \pm 11.6 MHz
Transmitter Pulse Length	0.5 μ sec
PRF	1600 pps
Power Output	60 KW
Power Amplifier	Magnetron
Receiver Dynamic Range	80 dB
Noise Figure	7.0 dB
Receiver	Linear
Receiver Dynamic Range	55 dB
Noise Figure	6.5 dB
Receiver B.W.	2 MHz
Intermediate Frequency	30 MHz
Antenna Polarization	Linear, Vertical
Beam Width	Horiz. 1.35 $^{\circ}$; Vert. 1.9 $^{\circ}$
Gain, Main Beam	40 dB
Sidelobe Gain	23 dB down
Azimuth Coverage	\pm 50 $^{\circ}$
Elevation Coverage	360 $^{\circ}$
Stabilization	Ground Track, Pitch and Roll
Unambiguous Range	51.9 Nmi
Unambiguous Velocity	\pm 12.9 m/sec

TABLE 1
Radar Characteristics

turning the coherent oscillator on at the same time during each transmitter pulse the reference is generated which is necessary to measure the Doppler shift in the returns from radar reflectors. The output of the coherent oscillator is sent to a quadrature coupler. The coupler will produce outputs that have a 90 degree phase relationship. The unshifted and shifted phase signals are applied as one input to the phase detectors.

During the radar interpulse period any return signal is coupled through the RF circulator to the RF preamplifier. The RF preamplifier has two functions. One is to amplify the returns signals for good power splitter operations. The second is to aid in reducing the system noise figure. The power splitter will divide the power at its input equally between the linear and logarithmic receiving channels. The logarithmic receiving channel will amplify and detect the return signals for dBZ measurements. The signal for the power splitter that is coupled to the mixer preamplifier is mixed with the output of the stable oscillator. The IF output of the mixer preamplifier is amplified by the linear IF amplifier and applied to the phase detectors by way of a power splitter. The phase detectors now have as their inputs a signal that is coherent with the transmitted frequency and a signal return from a radar reflector that includes the transmitted frequency plus any Doppler frequency. The voltage output of the phase detectors is proportional to the phase difference of the signals applied to the phase detectors. The phase detector outputs are amplified for output to the data system.

2.0 Airborne Doppler Radar Error Sources

2.1 Transmitting and Receiving System Instabilities

The system described in the preceding section is patterned after the classical approach to a Moving Target Indicator (MTI) system. The

prime sources of system instabilities, which will produce errors in any Doppler data, are frequency instabilities in the transmitted pulse interval (τ), the stable oscillator, and the coherent oscillator. Additional errors which result from platform instabilities and transmitted RF beam characteristics will be considered later.

The signal transmitted by the radar is

$$A_1 (\cos \omega_{tr} t + \theta_{tr})$$

where ω_{tr} is the angular frequency at time (t) and θ_{tr} is the phase of the transmitted signal. A sample of the transmitted signal is mixed with the stable oscillator, whose output can be defined as

$$A_2 (\cos \omega_{so} t + \theta_{so})$$

where ω_{so} is the angular frequency at time (t) and θ_{so} is the phase of the stable oscillator. The mixed signals will produce an intermediate frequency (IF), of

$$A_3 \cos ((\omega_{tr} - \omega_{so}) t + \theta_{tr} - \theta_{so}).$$

The IF signal has preserved the frequency and phase characteristics of both the transmitted signal and the stable oscillator. The coherent oscillator senses a positive going voltage change in the magnetron output, mixed to IF, as a signal to turn the coherent oscillator on. On each transmitted pulse, the coherent oscillator will sense the same voltage level and the oscillator will each time start its oscillator with the same phase. The output of the coherent oscillator can be described as

$$A_4 \cos (\omega_{co} t + \theta_{tr} - \theta_{so} + \theta_{co}).$$

Where θ_{co} represents the error in the phase locking.

The phases of the combined transmitted signal and the stable oscillator signal are carried through to the output of the coherent oscillator.

Any echo from a fixed target at range R will arrive back at the radar in the form of

$$A_5 \cos (\omega_{tr} t - \omega_{tr} T_0 + \phi_{tr})$$

where T_0 is the time it takes for the transmitted energy to reach the target and return.

$$T_0 = 2R/c.$$

The return echo signal is mixed with the stable oscillator frequency to produce an IF of

$$A_6 \cos ((\omega_{tr} - \omega_{so}) t + \phi_{tr} - \phi_{so} - \omega_{tr} T_0).$$

The return IF signal is mixed in a phase detector with an in-phase component of the coherent oscillator output producing

$$k \cos ((\omega_{tr} - \omega_{so} - \omega_{co}) t - \omega_{tr} T_0 + \phi_{co})$$

and also the quadrature component of the coherent oscillator to produce

$$k \cos ((\omega_{tr} - \omega_{so} - \omega_{co}) t - \omega_{tr} T_0 + \frac{\pi}{2} + \phi_{co})$$

If the coherent oscillator is perfectly phase locked to the combined transmitted signal and the stable oscillator signal then the term ϕ_{co} would vanish. Also, if the coherent oscillator frequency were perfectly fixed to the difference between the magnetron and stable oscillator, then the expressions for the output signals would reduce to

$$k \cos \omega_{tr} T_0 \quad (1) \text{ and}$$

$$k \cos \omega_{tr} T_0 + \pi/2 = k \sin \omega_{tr} T_0$$

As long as the distance to the target return is constant, the output of the phase detector will be at a fixed amplitude. However as the distance between the transmitter and the echo changes, the amplitude of the signal from the phase detector will vary between $\pm k$.

(1) Barton, David K. "Radar System Analysis" pages 199-219, Prentice-Hall, Inc., Englewood Cliffs, New Jersey.

In the case of the system described, the coherent oscillator is phase locked to the resultant transmitter plus stable oscillator frequency but is not frequency locked. So the output of the phase detector will be

$$k \cos (\omega_{tr} (t - T_0) - (\omega_{so} + \omega_{co}) t + \theta_{co})$$

Let the transmitted pulse be positioned anywhere in the pulse repetition interval such that

$$T_0 \leq t \leq T_0 + \tau_p \quad \tau_p = \text{transmitted pulse width}$$

At the beginning of the transmitted pulse and substituting for t we have

$$k \cos (-(\omega_{so} + \omega_{co}) T_0 + \theta_{co})$$

at the end of the transmitted pulse interval, we have

$$t = T_0 + \tau_p$$

$$k \cos (\omega_{tr} \tau_p - (\omega_{so} + \omega_{co})(T_0 + \tau_p) + \theta_{co})$$

$$k \cos ((\omega_{tr} - \omega_{so} - \omega_{co}) \tau_p - (\omega_{so} + \omega_{co}) T_0 + \theta_{co})$$

Since the sum of $(\omega_{tr} - \omega_{so} - \omega_{co}) \approx 0$ and $T_0 \gg \tau_p$ the major contributors to phase errors will be the term $(\omega_{so} + \omega_{co}) T_0$ and the coherent oscillator phase error.

2.2 Internal Stability Requirements

By taking the output of the phase detector, the total phase instability can be lumped into three parts. The phase instability due to the stalo from one phase repetition period (t_p) to the next is

$$\Delta_{so} = \Delta\omega_{so} t_p$$

The phase instability due to the coherent oscillator is

$$\Delta_c = \Delta\omega_{co} t_p$$

The phase instability due to the transmitter will be

$$\Delta_{tr} = \Delta\omega_{tr}\tau_p$$

It would be a simple matter to predict the influence of each and the combined residues on the Doppler spectra if the residues were well behaved. This is not the case. Frequency drift, amplitude modulation, frequency modulations are neither always in the same direction nor at the same time. Also, it would be most difficult to include all factors that would influence the maximum value of the residues produced by each source. Because of the many variables involved it was determined that an empirical solution to test the stability would be sufficient.

Selection of the oscillators were made in accordance to a clutter rejection factor of 15 dB. Since, as shown by Sirmans,⁽²⁾ a signal-to-noise (clutter) ratio of 15 dB is sufficient for estimation of meteorological signal parameters. For the transmitter the intrapulse frequency change should be no more than⁽³⁾

$$I = 20 \log \left\{ \frac{1}{\pi \Delta f \tau} \right\}$$

$$\text{if } I = 15 \text{ dB}$$

$$5.62 (\pi) (\tau) = \frac{1}{\Delta f} \quad \tau = 0.5 \times 10^{-6} \text{ sec.}$$

$$\Delta f = 113.2 \text{ KHz}$$

$$\text{Operating frequency } 9.3 \text{ GHz}$$

$$\text{or } 12.17 \text{ parts per } 10^6 \quad \% \text{ change} = \frac{113.2 \times 10^3}{9.3 \times 10^9} = 0.0012\%$$

for the stable oscillator the frequency change over one pulse repetition interval should be no more than

$$I = 20 \log \left(\frac{1}{2\pi \Delta f T} \right) \quad T = 625 \times 10^{-6} \text{ sec}$$

$$\Delta F = 45.28 \text{ Hz}$$

(2) Sirmans, Dale and Bill Bumgardner, "Numerical Comparison of Five Mean Frequency Estimators" Journal of Applied Meteorology Vol. 14, No. 6, September 1975, pages 991-1003.

(3) Skolnik, Merrill I. "Radar Handbook" McGraw-Hill, Chapter 17 by William W. Shroder.

the oscillator operates at approximately 9.3GHz yielding a stability of .004869 parts per 10^6 (4.86 parts per 10^9 in 625 μ sec or 7.776 parts per 10^6 per second.)

the coherent oscillator should have a stability of at least

$$I = 20 \log \left(\frac{1}{2\pi\Delta f T} \right)$$

$$\Delta f = 45.28\text{Hz}$$

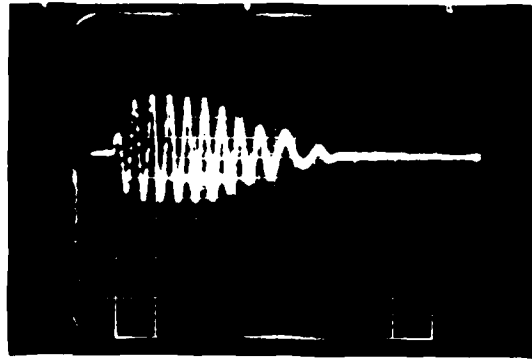
$\frac{45.28}{30 \times 10^6} = 1.5$ parts per 10^6 in 625 μ sec or 2.4 parts per 10^3 per second.

The magnetron used in the transmitting system has specifications for pulling figure of 5 MHz and a pushing factor of 1.0 MHz/Amp. The load on the magnetron will be constant during the tests but the magnetron current will be changing from the start of the transmitter pulse to its end. Figure 2 shows the result of mixing the transmitter pulse with a stable CW source. The estimate of frequency change in the tail end of the pulse is given in Graph No. 1. It is expected that the frequency deviation in the tail end of the transmitted pulse will result in an increased base line noise level.

Items that will be determined during the system tests are: (1) Is the system stable? (2) Does the noise level increase as a result of returned echoes containing the frequencies in the tail of the transmitted pulse? (3) Can the system be used in an airborne environment to measure radial velocities?

2.3 External Stability Requirements

The rate that the antenna rotates, the positioning error of the radar RF beam and the maintenance of the RF beam in space (stabilization) all contribute to the errors in the measurement of radial velocities.



→ Time

Figure 2. Single Transmitted Pulse Mixed With Stable Oscillator
Scale 0.2 m/sec per division

For the tests, all data will be taken with the antenna fixed in position such that stationary targets will have zero Doppler shift, however, platform motion due to aircraft position translation will result in an equivalent antenna scan which will widen the Doppler spectrum. The errors in the measurement of radial velocities can be grouped into two categories. One group consists of all errors that widen the Doppler spectra. The other group consists of the errors which cause the center of the spectrum to be shifted in frequency.

Antenna stabilization will produce both spectrum spreading and spectrum shifting. Antenna pointing errors will induce a spectrum shift because the antenna will not be positioned along a fixed target zero isodop. Instead the aircraft velocity component $V \cos \theta$ will enter into the measured velocities. V is the aircraft ground speed and θ is the angle between ground track and antenna pointing position. Stabilization errors which cause the antenna to hunt for a null result in broadening the RF beam. The broader the beam, the broader the measured spectrum.

The stabilization characteristics of the antenna assembly used are such that the worst case error in position will be one degree. If the antenna were perfectly stable but with a one degree pointing error then any radial velocity measured would have introduced into it an error of $\pm V_{a/c} \sin 1^\circ$. At 125 m/sec aircraft speed the error varied plus and minus one degree about the null point, the antenna beam width would be increased by two degrees. The apparent RF beam width increase would result in higher errors in the estimation of mean velocity from the variance producing mechanisms such as shear, beam broadening, and antenna rotation. Using a 1.35 degrees width, the velocity variance σ_v^2 is

the sum of σ_s^2 (variance due to shear), σ_b^2 (variance due to beam broadening), σ_r^2 (variance due to antenna rotation), σ_d^2 (variance due to drop size fall speeds), and σ_t^2 (variance due to turbulence). Using the equation given by Nathanson.⁽⁴⁾

$$\sigma_s^2 = 0.51(\text{m/sec})^2 \text{ at 8km range.}$$

$$\sigma_d^2 = 0.001(\text{m/sec})^2 \text{ when a 1m/sec vertical velocity component is used.}$$

The beam broadening term as given by Nathanson must be modified to include the speed of the particles relative to the aircraft.

$$\sigma_b^2 = \{0.42\theta_2 (v_w \sin \beta + v_{ac} \sin \gamma)\}^2$$

where

θ_2 = 2 way half-power beam width in radians.

v_w = mean wind speed.

β = angle of wind relative to beam center.

v_{ac} = ground speed of the aircraft.

γ = angle of beam relative to ground track.

When β and $\gamma = 90^\circ$

$$v_w = 12 \text{ m/sec}$$

$$v_{ac} = 125 \text{ m/sec}$$

$$\theta_2 = 0.0167 \text{ radians}$$

$$\sigma_b^2 = 0.926 (\text{m/sec})^2$$

Variance due to turbulence as estimated by Sirmans and Doviak⁽⁵⁾ can vary from 1 to 4 (m/sec)².

(4) Nathanson, Fred E. "Radar Design Principles" McGraw-Hill, 1969, pgs. 205-210.

(5) Sirmans, Dale and R. J. Doviak "Meteorological Radar Signal Intensity Estimation" pages 11-16.

With the antenna not rotating, the equation for variance due to antenna rotation is changed to use the aircraft translational motion for antenna time on target.

$$\sigma_r^2 = \left(\frac{v\lambda}{7.6d\theta_1} \right)^2$$

where v = a/c ground speed
 λ = transmitter wavelength
 d = distance from a/c
 θ_1 = horizontal beamwidth
 d = 10km
 v = 100m/sec
 λ = 0.032m
 θ_1 = 0.0236 radians

$$\sigma_r^2 = 3.19 \times 10^{-6} (\text{m/sec})^2$$

The expected variance in the velocity spectrum will vary from 1.978 to $4.978(\text{m/sec})^2$. Turbulence and beam broadening will be the largest spectrum spread components.

3.0 Test Program

The tests performed on the Doppler radar were to determine:

1. Are the transmitter and oscillators stable enough for Doppler measurements?
2. Will the system stability be maintained in an aircraft environment?
3. How well can the Doppler, when installed in the aircraft, measure the radial velocities in light to heavy precipitation and in non-turbulent to turbulent meteorological situations?

3.1 Test Description and Results

Initial tests of the Doppler radar were conducted with the radar fixed in position as a ground-based radar. System stability was estimated by observing fixed targets in the vicinity of the test site. The best targets available were the mountains to the west of Boulder, Colorado.

Figures 3a and 3b show repetitive sweeps of ground clutter. As can be seen in Figure 3b some amplitude instability is present in the figure. The instability is a result of the transmitter, coherent oscillator and stable oscillator. The ground clutter presentations when compared to clutter presentations taken from klystron tube type Doppler radars has shown that such instabilities will not compromise the radars ability to provide data for velocity measurements.

The second ground test was whether or not the noise level increase with detected targets would mask low level signals. Figure 4a shows the system noise level with no received signals. Figure 4b shows the Doppler spectrum of snowflakes and the increased noise level caused by the received signal. Again based on prior tests the increased noise level would not compromise the Doppler measurements.

The Doppler radar and its associated data system were installed in the WP-3D aircraft in May of 1978. The radar was installed in the tail of the aircraft so that observations could be made with the radar antenna pointed along a zero isodop. Flights were conducted on May 19 and May 30 at Miami, Florida, and June 8 and June 9 at Norman, Oklahoma.

During the tests out of Miami, Florida, chaff was used as a target. The chaff was both a good radar reflector and could be oriented optimally for the tests. Chaff was dropped in a line at an altitude of 10,000 feet (3048m). The chaff line was made as perpendicular to the prevailing winds as possible to optimize observable chaff movement. The aircraft tail antennas was perpendicular to the aircraft ground track to remove any aircraft speed influence on measurements. A race track pattern was flown around the chaff area at different ranges to check for system

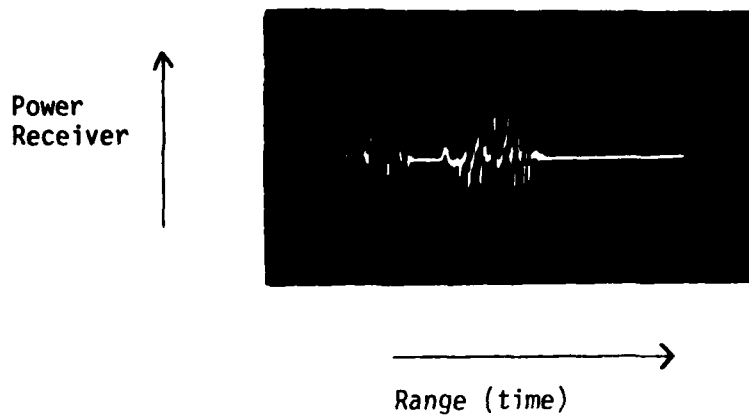


Figure 3a. Bipolar Video of Ground Returns Repetitive Transmissions (5 μ sec/div)

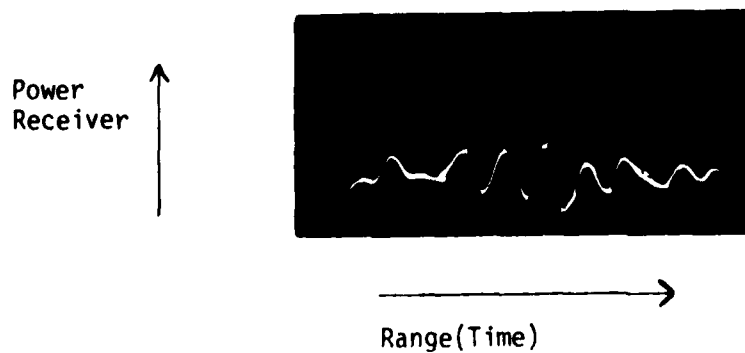


Figure 3b. Bipolar Video of Ground Returns Repetitive Transmissions (0.5 μ sec/div)

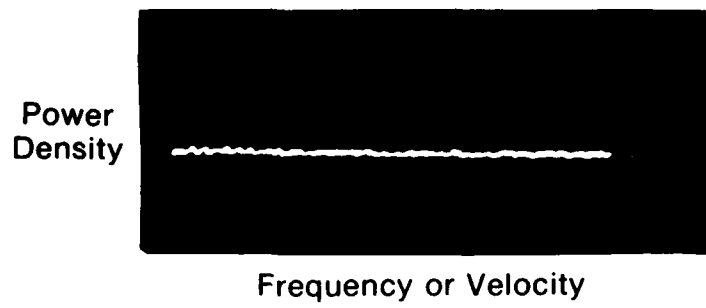


Figure 4a. Noise Level With No RF Returns

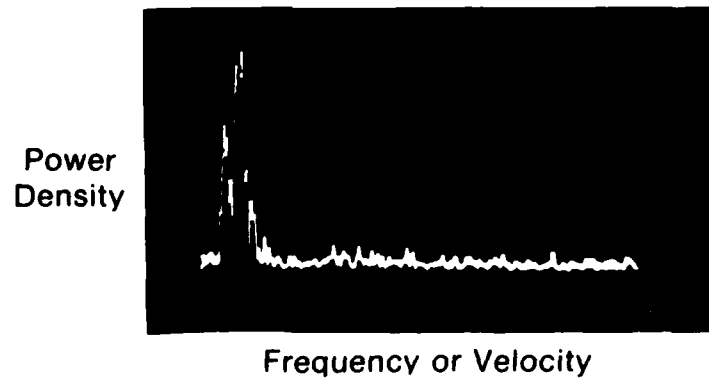


Figure 4b. Doppler Spectrum of Snow Flakes
with Increased Noise

stability as a function of range as well as velocity determination. (See Fig. 5.)

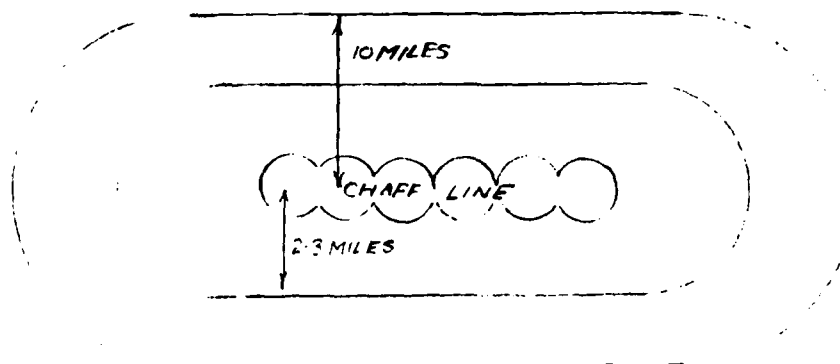


FIGURE 5
RACE TRACK PATTERNS

As an estimate of the winds in the area of the chaff drop, the inertial navigation system (INS) was used to measure the winds along the chaff drop line at the time that chaff was being dispensed from the WP-3D aircraft. Chaff 0.61 inches in length were dropped manually from the aircraft dropsonde chute. Chaff dispersion was a result of the air turbulence on the outside of the aircraft. Once the chaff was dropped, the aircraft began its race track pattern. The antenna was moved only in the elevation pointing direction while searching for the chaff.

In order to check the pointing accuracy and stabilization of the antenna assembly, the radar antenna was pointed down to measure the vertical velocity of the ocean surface with respect to the aircraft. As shown in Graph 2, Vertical Velocities, the velocities measured by the aircraft INS and the radar system are well within an expected error of two meters per second. The average velocity measured and calculated by the Inertial Navigation System is 0.18 meters per second with a standard

deviation of 0.74 meters per second. The average velocity measured by using the doppler radar is 0.05 meters per second with a standard deviation of 0.8 meters per second. Measurements for the data set were taken with the aircraft flying at an altitude of 3450 meters (11,318 feet). Graph 2a, Ground Clutter Radial Velocity vs. Commanded Antenna Position, shows a comparison between the calculated ground clutter radial velocities and the same velocities measured using the Doppler radar. The objective of the data set was to determine if the antenna stabilization system for aircraft pitch, roll and drift angles was correcting the antenna position. There is an almost constant offset in the measured data from the calculated. The offset average velocity is 1.06 meters per second. Once the offset is known, it can be removed in future data reduction.

From the test flight conducted on May 30, 1978, out of Miami, Florida, two conditions were reviewed as follows: Graph 3 shows the aircraft positions during the chaff drops and one segment of the observation period. The chaff drop line is approximately 45 km (25 NM) in length and at an altitude of 3445 meters (11,300 ft.). The distance from the chaff to the aircraft observation position is approximately 14.4 km (8 NM). Graph 4 shows the wind speed as measured by the aircraft instrumentation during the times that chaff was being dropped and during the observation periods. The winds were very light. However, the Doppler measured winds were within the expected range of the aircraft measured winds. The large deviation in the Doppler radar data can possibly be attributed to having to move the radar antenna in tilt to maintain an optimum radar target. The average wind speed measured by the aircraft instrumentation was 1.8 meters per second with a standard deviation of 0.7 meters per second. The Doppler radar measured average values for wind speed is

0.65 meters per second with a standard deviation of 1.08 meters per second. It is not expected to have an exact correlation between these data sets. One reason is that a significant time lapse exists between the data sets. Another reason is that the present data system does not take into consideration the aircraft attitude parameters that are available for use in data correction schemes. A data system design for the airborne Doppler radar would have the necessary interface to the Inertial Navigation System to obtain aircraft attitude information for automatic correction of the Doppler radar data.

For the two flights in Oklahoma, the second flight on June 9, 1978, will be discussed. Chaff was used as a radar target to supplement the limited available weather targets in the Norman, Oklahoma, area. Graph 5 shows the chaff drop line and the position of the aircraft during the observation periods. The chaff line was approximately 36 kilometers (20 NM) in length. The chaff was dropped at an altitude of 2850 meters (9300 feet) and the observation altitude of the aircraft was 1332 meters (4370 feet). The sets of wind speed data as shown in Graph 5 indicate good correlation between the aircraft measured wind velocities and the Doppler radar measured radial velocities. The aircraft measured winds at the time chaff was being dispensed had an average value of 6.59 meters per second with a standard deviation of 0.75 meters per second for the first observation period and an average speed of 5.5 meters per second and a standard deviation of 0.53 for the second observation period. Graph 5 shows that the aircraft observation track is approaching the original chaff drop line. The rate of approach to the chaff could not be determined exactly due to the non-uniformity of the edge of the chaff line. Estimation of the approach speed is 3.5 meters per second,

based on the original chaff line. The Doppler radar measured values had an average velocity of 4.38 meters per second with a standard deviation of 1.04 meters per second for the first period and an average velocity of 4.73 meters per second with a standard deviation of 1.79 meters per second for the second period. It was observed that large deviations from the aircraft measured velocities occurred at the points that the chaff was first observed. The deviations can be attributed to the antenna being moved to optimize the chaff return signal. The major difference between the winds measured by the INE and the Doppler measured radial velocity was caused by the aircraft approaching the chaff line.

The data taken on meteorological targets is summarized in Figure 6. The aircraft's flight path was such that the aircraft flew between National Severe Storm Laboratory's (NSSL) radar and the area under observation. The area where common observations were made is located in the northwest section of Figure 6. The mean velocity over the area measured by NSSL's Doppler radar was -5.41m/sec with a standard deviation of 0.47. The mean velocity as determined by the airborne doppler radar was -4.9m/sec with a standard deviation of $1.77/\text{sec}$. The correlation between data sets is very good. The predominate factor for difference in the mean volocities is the areas of integration by the RF beams. Due to target range differences, the sampling area as seen by the airborne radar is approximately one fourth the area sampled by the ground based radar.

Additional data of interest are shown in Figures 7 and 8. The figures are representative of the quick look, processed on the ground, data printouts from the airborne Doppler radar data. Figure 7 shows the

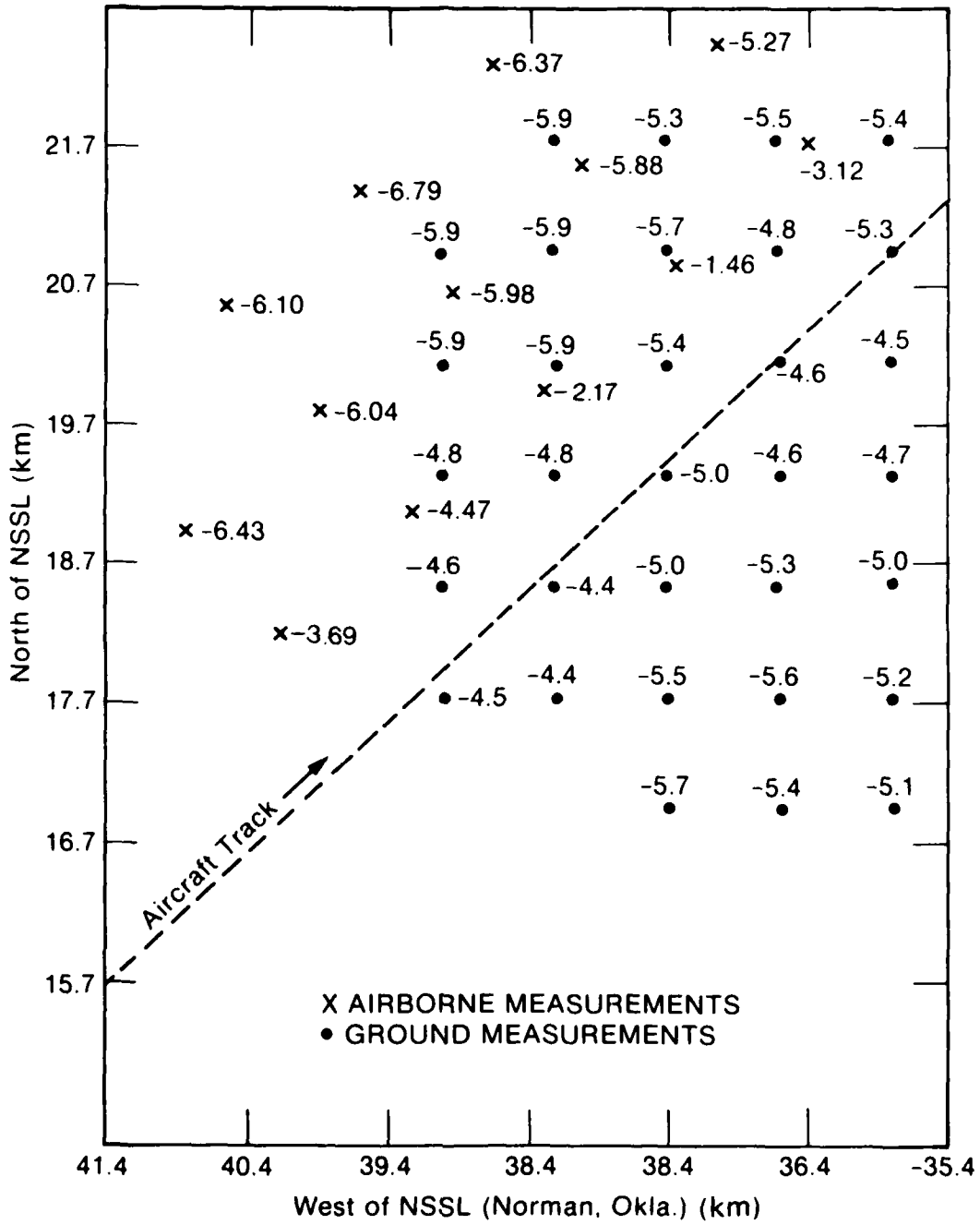


Figure 6. Doppler Data Fields
(Airborne and Ground Radars)

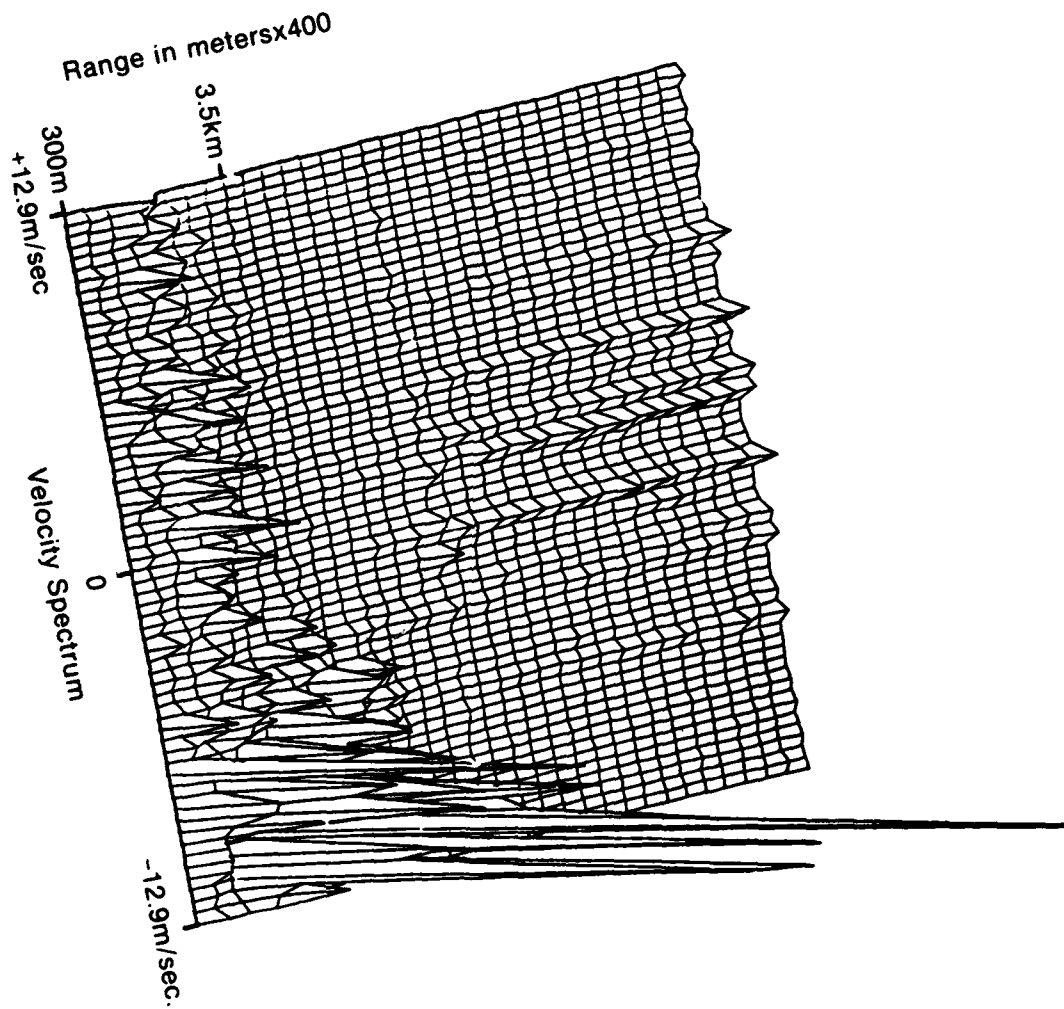


Figure 7. Velocity Spectrum of Rain

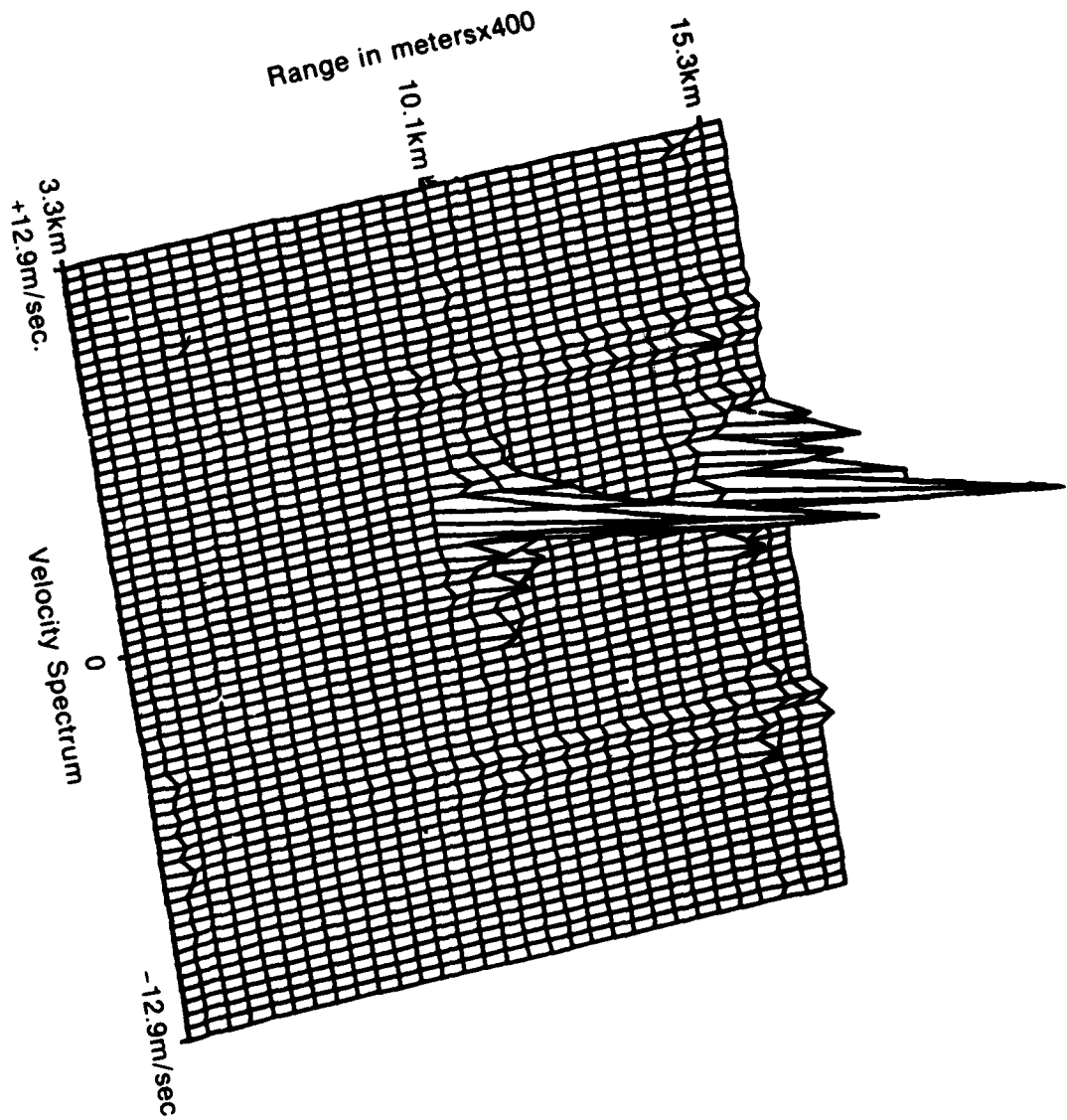


Figure 8. Range Velocity Spectrum of Chaff and Cloud

velocity spectrum of a heavy rain at the Miami Airport. The WP3D was sitting on the ground and the airborne Doppler radar antenna was pointed vertically at the falling rain. From the velocity spectrum it can be seen that the velocity of the droplets range from approximately -6.2 meters per second to -12.07 meters per second from particles observed at ranges of 700 meters to 3.5 kilometers. These measured values correlate well with the 9m/sec average reported by Nathanson⁽⁶⁾ for heavy rain. Figure 8 shows chaff that was detected while the aircraft was airborne. The chaff is at a range of 10.1 kilometers and has a radial measured velocity of approximately +3.08 meters per second. A cloud which is located behind the chaff and at a range of 15.3 kilometers has a measured radial velocity distribution of zero to +3.75 meters per second. The printouts were made by the National Center for Atmospheric Research Field Observation Facility from the radar data that was recorded on their data system which was loaned to us for the initial flight tests. A description of the data system is in Appendix I.

4.0 Conclusions

The questions that were to be answered by the tests are:

1. Is the system stable?
2. Does the noise level increase as a result of returned echoes containing frequencies in the tail of the transmitted pulse?
3. Can the system be used in an airborne environment to measure radial velocities?
4. How well can the Doppler, when installed in the aircraft, measure the radial velocities in light to heavy precipitation and in non-turbulent to turbulent meteorological situations?

⁽⁶⁾ Nathanson, Fred E. "Radar Design Principles" McGraw-Hill, 1969, pg. 210.

The first question was adequately answered via the ground tests. The observation of a fixed target did show that some instability was present in the system but the amount of instability did not prohibit measuring radial velocities. The base line noise level in the system did increase whenever video returns were present. The minimum detectable signal at the system output was approximately minus 100 dBm. At no time during the testing was it found that the system noise was masking a target whose radial velocities were to be measured. The results of the test have shown that the system can indeed be used in an airborne environment. There are some limitations on the system that must be considered when it is being used. The limitations are: (1) The antenna stabilization system is one of the more critical parts of the system. Errors in velocity measurements will occur if the exact antenna spatial pointing angle is not known. The magnitude of error in the measurement is a function of the error in the known antenna position and the ground speed of the aircraft. (2) The radar antenna RF pattern is somewhat prohibitive. The beam width will certainly add to the spreading of the velocity spectrum. But of more importance are the side lobes of the antenna RF pattern. Signals received via the side lobes will be summed with the signal received in the main beam. The side lobe returns from the ground could easily mask signals received from the main beam. Therefore, the airborne Doppler radar user must be aware of the antenna pattern through the radome, the attitude of the aircraft and the antenna pointing angle. (3) The transmitter-receiver system must be designed with an improvement factor of at least 15dB.

The last question to be answered has to do with the accuracy of the Doppler measurements. The estimation of measurement accuracy was $\pm 2\text{m/sec}$.

The vertical velocity measurements made with the aircraft Inertial Navigation Equipment (INE) and the Doppler radar showed that the two measurements were within a meter per second of each other. The comparison of the mean winds measured by the INE and those measured by the Doppler radar, with chaff as a target, showed that a difference of less than 2m/sec exists between measurements. The comparison, that was made between the wind field generated from data taken by the National Severe Storms Laboratory and the same field taken from data generated by the airborne Doppler radar, has shown that a difference of less than 1m/sec existed in the average winds in the two data sets. It is concluded that the radial velocities measured by the airborne Doppler radar will have an error of less than the estimated ± 2 m/sec figure. Situations did not exist to determine system usability in varying levels of turbulence. Additional testing will be required to provide an answer.

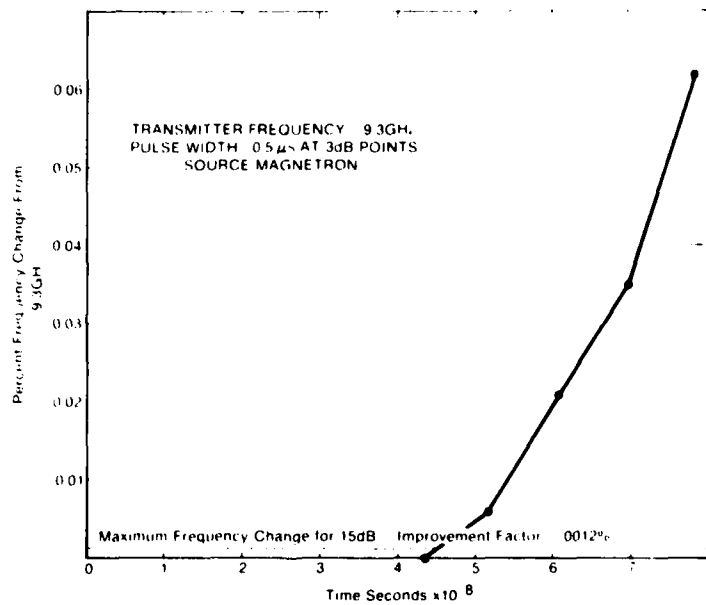
5.0 Recommendations

Based on the success of the data sets taken, it is highly recommended that the program be continued. The information taken to date has shown that the airborne Doppler radar for meteorological use is a realistic instrument that can and should undergo further development both for the scientific community and the general aviation community. The continuance of the program would necessitate that a semi-permanent radar installation be made on an aircraft so that needed data could be taken when the opportunity presents itself. This installation would eliminate the hazards of trying to schedule test times based on statistical possibilities of adequate weather at a particular location. However, all scheduled tests should not be eliminated. There still exists a great need for extensive ground truth data. This is, data, when taken concurrently

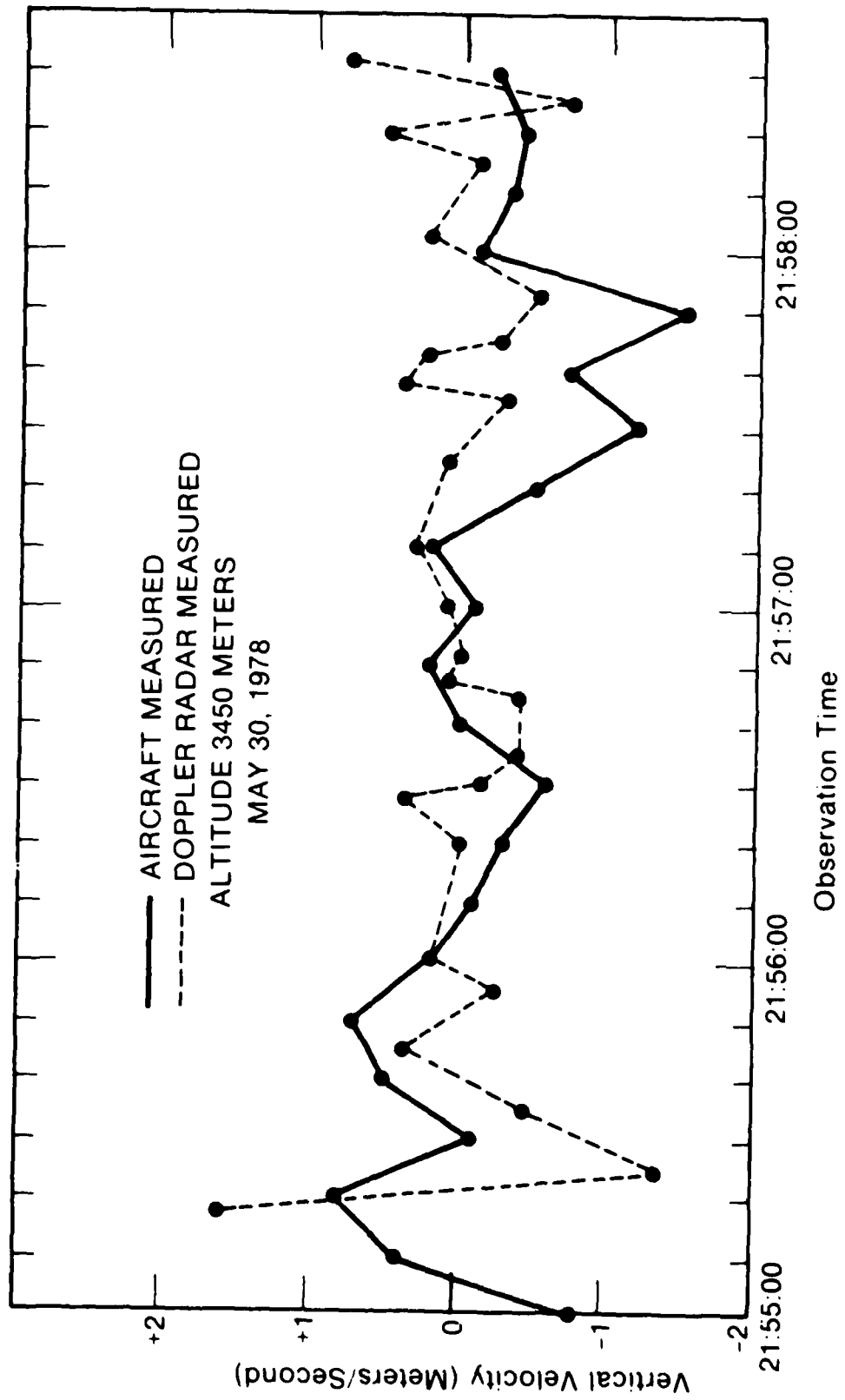
with a ground based Doppler radar and the airborne Doppler radar, that can be explained. Additional tests must be organized to learn the utilities of the Doppler radar. Application and application improvement can only come about by the instrument use in differing environments. Therefore, tests on a scheduled and non-scheduled basis should be carried out starting with stratiform situations, going to stratiform with imbedded cumulus then to cumulus.

In addition to the system application and learning process, the system equipment development must continue towards system optimization for aircraft use. The data equipment designs to date have been made with the idea that the equipment would be used on the ground in a fixed position. The aircraft application means that equipment miniaturization and hardening must be undertaken. Display systems must be developed to fit the application. Primarily, a display to reflect areas of turbulence and the degree of turbulence that the aircraft pilot or scientist can interpret in real time.

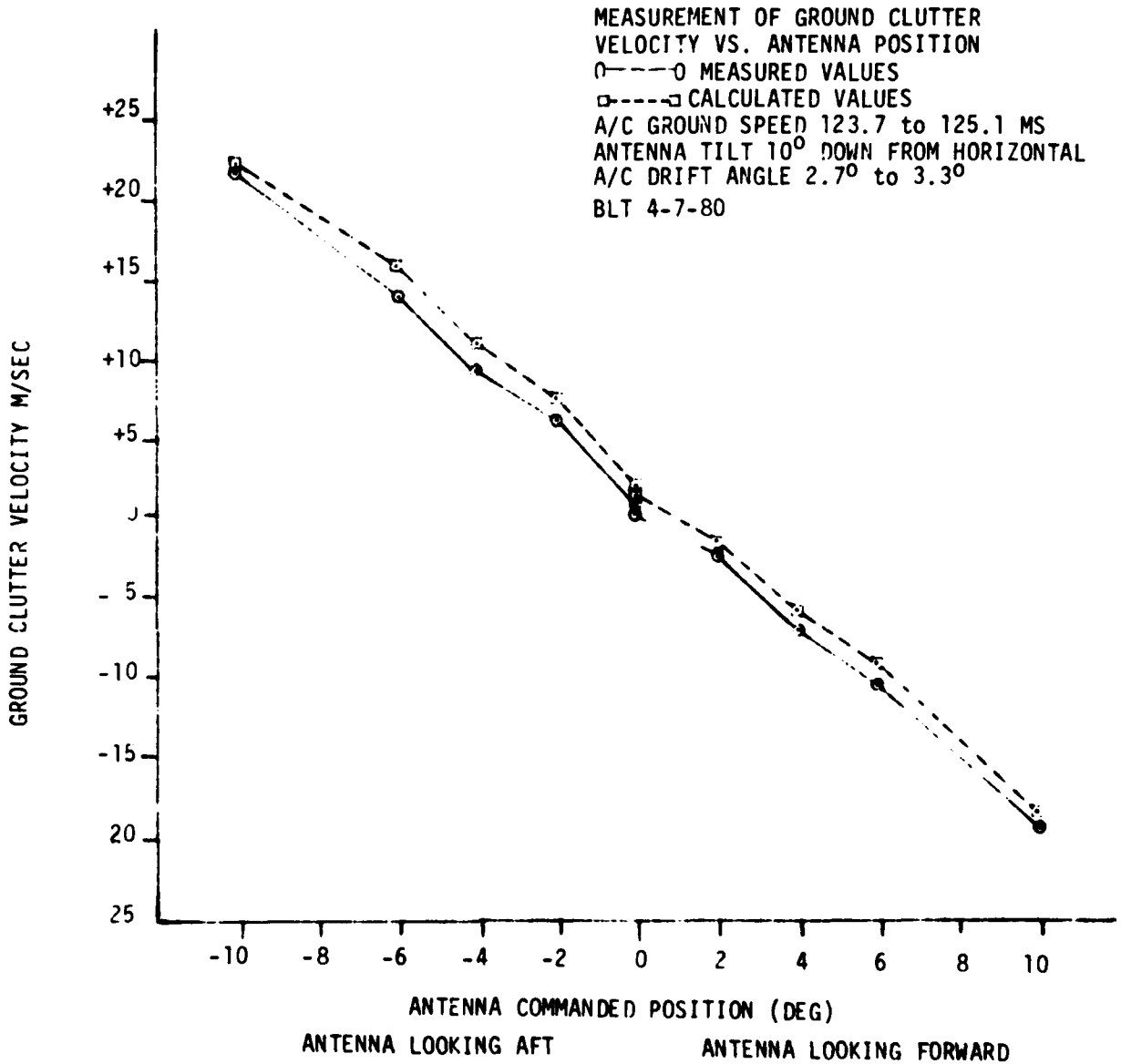
Therefore, this recommendation for program continuance is based on (1) the success of the test programs in acquiring useful data that demonstrates that an airborne Doppler radar for meteorological use is a realistic objective; (2) the need for a meteorological Doppler radar does exist for the scientists to explain the meteorological phenomena of systems that are reachable only by using an airborne remote sensor; and (3) the need exists for the commercial air carriers to be able to detect areas and severity of turbulence that if avoided could save countless dollars in airframe damage, and produce a greater margin of safety for air travelers.



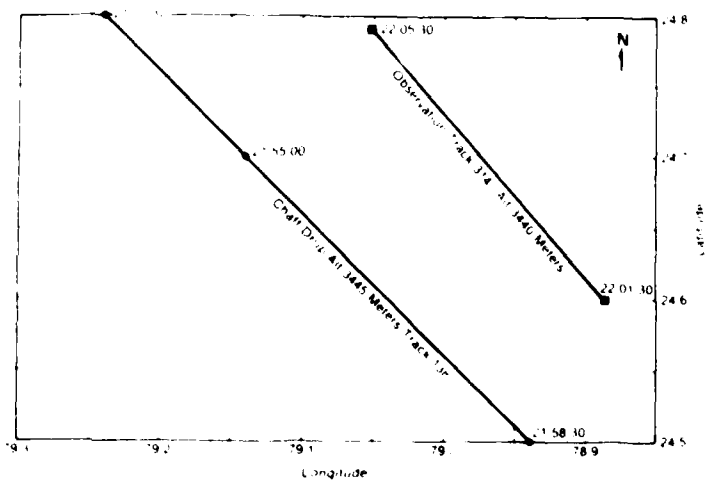
Graph 1. Percent Frequency Change in Transmitted Pulse vs. Time



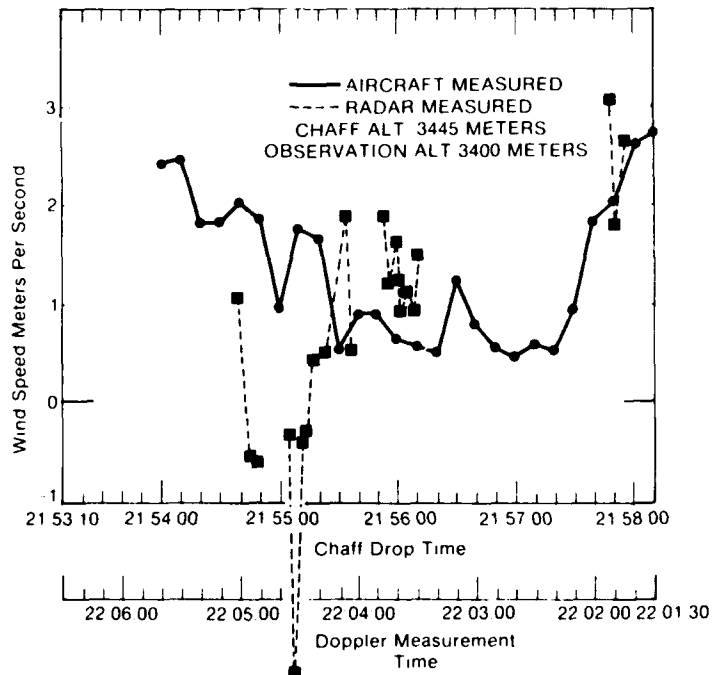
Graph 2. Measured Vertical Velocities



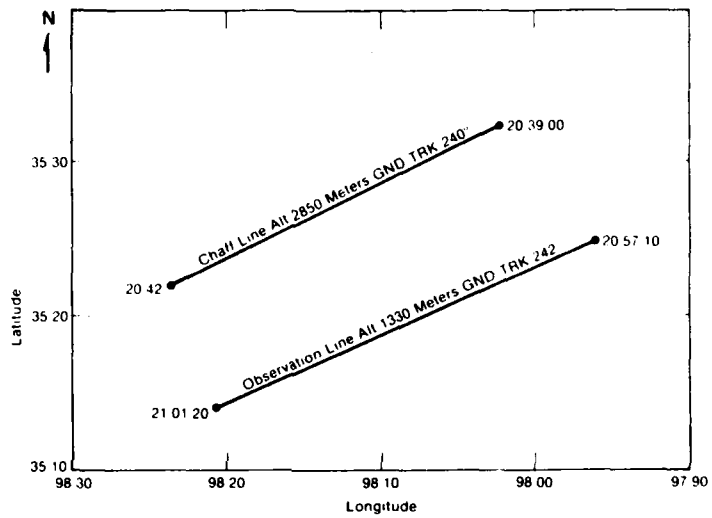
Graph 2a. Measurement of Ground Clutter Velocity vs Antenna Position



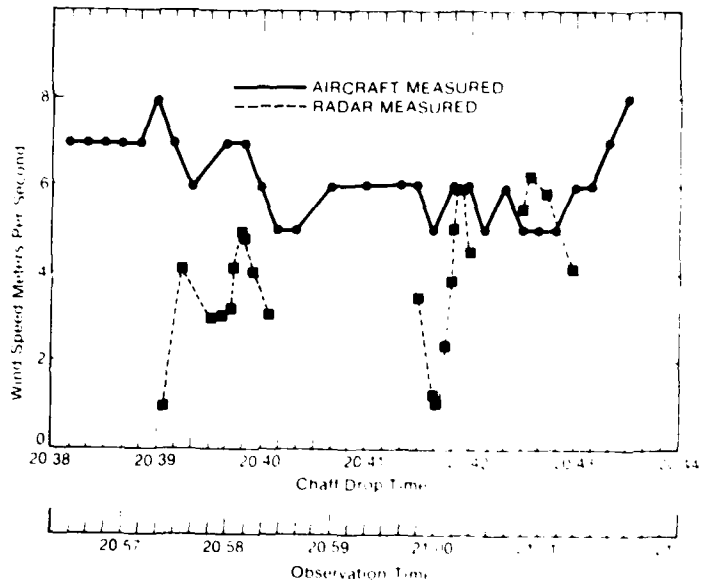
Graph 3. Aircraft Track During Chaff Drop



Graph 4. Wind Speed Measured by Aircraft During Chaff Drop



Graph 5. Chaff Drop in Oklahoma



Graph 6. Wind Speed Data

Appendix I. Description of the National Center for Atmospheric Research
Data System

NCAR / FOF

DATA ACQUISITION SYSTEM

Specifications:

INPUT:

Range: 10 nA to 200 ma, 100 microvolts to 0.5 Volt Recording Range
Bandwidth: D.C. to 20 MHz, +0, -3db: With offset corrector .01 Hz to 20 MHz
Overload Recovery: Recovers in less than 200 ns to .1% from a X100 current overload, if the maximum current is less than 1 amp.
Impedance: 10 ohms, 100 ohms, 1000 ohms, 10k ohms, depending on shunt setting.
Impedance settling time: less than 100 ns for X10 change.
Common Mode Rejection: -80db, DC to 1 MHz. -60 db at 5 MHz, -40db above 10 MHz with matched input cables.
Differential impedance error: less than .1% DC, less than 1% at 10 MHz.
Direct Sample and Hold Input: 50 ohms, \pm 5 volts

SAMPLE AND HOLD:

Option 1: Integrating Sample and Hold with 50 ns reset time.
Timing Range: Sampling Aperture time, 50 ns to 1000 ns, eight steps.
(range can be internally modified up to 10 millisecc.)

Specifications: (cont'd.)

SAMPLE AND HOLD

Option 1: Integrating Sample and Hold with 50 ns reset time. (cont'd.)

Timing Accuracy: Controlled by a 20.00000 MHz crystal oscillator. (15 MHz optional)

Timing Jitter: Sampling Aperture, less than 1 ns.

Sampling Interval, 2 ns worst case, less than 1 ns typical.

Systematic Aperture Width Error: 5 ns max, 2 ns typical.

Sampling Rates: Each Sample and Hold, 50 Hz to 5 MHz;

Interlaced Single Channel Mode using 2 Sample and Holds, 100 Hz to 10 MHz.

Amplitude Resolution: Better than -60db with apertures greater than 500 ns.

0.05% Full scale accuracy.

Option 2: Track and hold type Sample and Hold. (Ultra high speed.)

Aperture: 20 nanoseconds.

Aperture Jitter: Less than 200 picoseconds.

Feedthrough: .1 picofarad, Less than 1% at 10 MHz.

A/D CONVERTERS:

Option 1: 1 MHz 10 bit ultra linear A/D (Two used).

Method of conversion: Successive Approximation

Conversion time: 800 ns. (Data throughput at maximum rate: 10 megabit/sec.)

Specifications: (cont'd.)

A/D Converters: (cont'd.)

Option 1: Speed-Resolution product: 1×10^9 (a figure of merit)

Option 2: 5 MHz or (10 MHz) 8 Bit fast A/D (2 used)

Method of conversion: Modified Parallel, 4 bits at a time.

Conversion Time: less than 200 ns. (less than 100 ns)

Data Throughput at maximum rate: Over 40 megabits/sec. (80 megabits/sec.)

Speed-Resolution product: 1.3×10^9 (2.6×10^9) (a figure of merit)

TRIGGER:

Dual Slope DC Schmidt trigger with ± 40 V level control.

Trigger Bandwidth: 20 MHz.

Trigger Jitter: 20 microvolts (low range) 200 microvolts (high range)

With 1000 V/microsecond risetime 10V pulse, jitter is less than 2 ns.

Input Impedance: 200 ohms/2K ohms

Delay Option: Externally presettable from 0 - 999 increments.

Increments are internally selected from 100 nanoseconds to 1 millise.

Memory Data Blocking: Options to store 8, 16, 32, 64, 128, up to 2048 A/D conversions each time the system is triggered. Automatic transfer to the summing memory when the fast memory is full. Trigger lockout prevents timing reset while data is being recorded.

Special Doppler Mode: To allow maximum resolution in the recorded Doppler spectrum, special timing logic allows sequential filling of both memories with almost no dead time, followed by a double record output to tape. This allows recording up to 256 complex samples at 4 range gates, or as few

TRIGGER: (cont'd.)

Special Doppler Mode: (Cont'd.)

as 16 complex samples at 128 range gates, so that a FFT transform can yield spectral information from a group of returns taken in a very short time span, eg. 10 - 1000 milliseconds.

OUTPUTS:

TAPE: Output is 18 bit word containing 15 data bits, and 3 scaling information bits. A selector allows recording data bits 1 - 15 or bits 6 - 20 plus the scaling bits from the 24 bit summing memory.

Format: Each word is divided into three 6 bit bytes. The most significant bit (MSB) is recorded first in channel "B" on the tape, the LSB is recorded in the third byte in channel "1". (Using 7 track IBM notation)

Record Length is variable in increments of 8 words (24 bytes) up to 2048 words. In addition, a 60 byte header containing housekeeping and system data is written on tape prior to the data bloc.

Timing: Either synchronous or incremental. Any synchronous tape drive can be connected to the system. Any incremental recorder or punch can be used. Maximum data transfer rate is 6 megabytes/sec.

Analog Outputs:

10 Bit 25 ns D/A with 50 ohm output amplifier monitors contents of fast input memory which cycles continuously through the memory at the data logging rate when not triggered.

10 Bit 150 ns D/A with 50 ohm output amplifier monitors any 10 bits of the summing memory which cycles at 100 KHz word rate in the display mode. Front panel option exists for cycling the summing memory at the data logging rate even in the display mode, up to a maximum rate of 2 MHz word rate. Front panel data selector determines which bits are displayed, allowing the output display to represent the data stored divided by 2^N where N is any number from 0 to 10, except 7 and 9.

Synchronizing Outputs:

Two synchronizing outputs are provided on the front panel which provide a pulse

Specifications: (cont'd.)

Synchronizing Outputs: (cont'd.)

when the address to each of the memories is "1". This allows a scope to be triggered on the beginning of a data frame.

An additional output is provided on the back which is high whenever the system is storing data in the fast memory. This allows the operator to see what portion of the return he is recording.

A clock output at the sampling interval rate is available on the rear panel

Gain-Switching Preamp Outputs:

50 ohm outputs are provided from both gain-switching preamps. These outputs also serve as direct sample and hold inputs.

HOUSEKEEPING DATA SYSTEM:

Permanent Inputs: Day of Year, Time of Day, (Hours, Minutes, and Seconds generated from an internal crystal clock, accurate to better than 1 second a day.)

Sampling Aperture, Sampling Interval, Record Number, Number of shots summed in the record, Trigger delay, Number of range gates recorded per input trigger.

Scanning and Location Information: system latitude and longitude, (degrees, minutes),

Pedestal pointing azimuth and elevation, (or aircraft attitude), (Degrees only).

Miscellaneous Data: Temperature, Calibration code for offset or attenuation data, transmitter power, miscellaneous input thumbwheel.

READOUT AND DISPLAY SCHEME:

The readouts are strobed in groups of ten digits, six at a time.

The same strobe circuit cycles six mod 10 shift registers containing the stored housekeeping data. New data may be entered into the registers at any time, allowing the system to interrogate another system, such as a navigation computer, or collection of sensing devices.

When a readout onto tape is initiated, timing control is transferred to the acquisition system, which then strobes out the data into the formatter.